Phase Transition of the Lennard-Jones System. II. High-Temperature Limit

Jean-Pierre Hansen

Laboratoire de Physique Théorique et Hautes Energies, 91-*Orsay*, *France**

(Received 4 February 1970)

The high-temperature part of the fluid-solid coexistence curve for Lennard-Jones systems is investigated by "exact" Monte Carlo calculations. The interaction potential is separated into its repulsive ($4/r^{12}$) and attractive ($-4/r^6$) parts. The repulsive part is treated "exactly" by Monte Carlo computations with a 864-atom system, and the attractive part is treated as a perturbation. The "unperturbed" potential, which is homogeneous in the coordinates of the interacting particles, has trivial scaling properties which greatly simplify the computations. The attractive perturbation is treated to first order; the second-order corrections are shown to be very small at not-too-low temperatures. A high-temperature equation of state is obtained for the Lennard-Jones fluid, which is in excellent agreement with exact Monte Carlo computations at temperatures as low as about twice the critical temperature. Using the Hoover-Ree scheme, the free energy of the solid is determined and the transition densities and pressures calculated in the first-order approximation, which is shown to be quite satisfactory. The validity of Lindemann's melting "law" and a crystallization criterion based on the maximum of the structure factor are investigated.

I. INTRODUCTION

One of the recent successes of "computer-experiment" techniques applied to classical systems of atoms interacting through "realistic" two-body forces, has been the study of first-order phase transitions.[1-5] In Ref. 2, Hoover and Ree proposed an ingenious method for the exact determination of the fluid-solid transition data. The free energy of the fluid phase is readily evaluated by integrating the equation of state computed by a Monte Carlo[6] or a molecular dynamics[7] procedure. Hoover and Ree showed that the solid-phase free energy could be calculated by integrating the single-occupancy (cell-model) equation of state computed by a modified Monte Carlo procedure where each atom is confined to its own cell of volume $v = V/N$; here V is the total volume of the system, N the total number of atoms of the order of several hundred in calculations done on the currently available fastest computers. In Ref. 3, Hoover and Ree applied their method to the fluid-solid transition of hard disks and hard spheres. The same method was applied by Hansen and Verlet[4] (this paper will hereafter be referred to as I) to the melting transition of systems of atoms interacting through the two-body Lennard-Jones (LJ) potential

$$v(r) = 4\epsilon\,[(\sigma/r)^{12} - (\sigma/r)^6] \quad . \tag{1}$$

In I, a similar method, based on a limitation of the density fluctuations, was applied to the study of the condensation transition. The transition data along four isotherms ranging from the triple-point temperature to about twice the critical temperature was thus obtained and shown to be in good agreement with argon data if the potential parameters ϵ and σ are given those values which fit the second virial coefficient at not-too-low temperatures,[8] i. e., $\sigma = 3.405$ Å, $\epsilon/k = 119.8$ °K. If quantum corrections are included, the agreement with neon data, using the parameter values ϵ and σ determined under 0 °K conditions,[9] has been shown to be equally good.[10]

It must be stressed, though, that the computations leading to the phase transition data for LJ systems are rather costly, as complete-fluid and single-occupancy equations of state must be generated along several isotherms. On the other hand, if one is interested in the high-temperature transition data, a perturbation approach in powers of $\beta = 1/T$ can be expected to yield reasonable results. These considerations led us to investigate systems interacting solely through the repulsive $4\epsilon(\sigma/r)^{12}$ part of the LJ potential, the attractive part $-4\epsilon(\sigma/r)^6$ being treated as a perturbation. The unperturbed potential being homogeneous in the coordinates of all the atoms, a simple scaling procedure allows one to deduce results at various temperatures and densities from the data computed along a single isotherm. On the other hand our detailed numerical calculations which will be presented here, show that including only the first-order perturbation correction to various thermodynamic quantities yields very satisfactory results at not-too-low temperatures (more precisely temperatures ranging from about twice the critical temperature upwards). Thus the complete high-temperature part of the coexistence curve for LJ systems can be computed if the inverse-12 potential problem has been numerically solved for a single value of β. Similar calculations have been

done independently by Hoover and collaborators,[5] who did not, however, study the effect of the attractive inverse-6 part of the potential. Their results for the inverse-12 potential (or "soft sphere") problem are in remarkable agreement with our data.

The second purpose of this work was to check the validity of two empirical laws which predict the melting and crystallization densities from properties of one of two coexisting phases. The first of these laws is the time-honored Lindemann melting law which we checked primarily in the low-temperature region. The second law is a criterion based on the height of the first peak of the structure factor in the fluid phase and is discussed in I where it was shown to hold in the temperature range considered in that work. Here we shall discuss its extension into the high-temperature region.

The inverse-12 potential problem and inverse-6 perturbation are briefly discussed and all relevant formulas written down in Sec. II. The numerical results from our Monte Carlo computations are presented in Sec. III. The melting and crystallization criteria are discussed in Sec. IV where their validity and limitations are examined. Some concluding remarks are given in Sec. V.

Throughout this paper all quantities will be expressed in reduced units, i.e., units where $\sigma = \epsilon/k = 1$. Densities (denoted by ρ) are expressed in atoms per unit volume (i.e., atoms$/\sigma^3$); note that these densities are the same as those used by Hoover *et al.* which are taken relative to the density at which hard spheres of diameter σ' would be close packed; the σ' of Hoover *et al.* and our σ differ by a factor of $2^{1/6}$.

II. INVERSE-12 POTENTIAL PROBLEM AND PERTURBATION THEORY

Consider a system of N atoms interacting through the LJ potential Eq. (1). The configurational part of the partition function reads

$$Q_N = \frac{1}{N!}\int_V \exp\left[-\beta \sum_{i<j} v(r_{ij})\right] d^3r_1 \cdots d^3r_N . \tag{2}$$

At high temperatures ($\beta \ll 1$) the atoms penetrate deeply into the repulsive "cores" of their neighbors and for small interatomic distances ($r < 1$), the inverse-12 term of the potential clearly dominates the inverse-6 term and it is reasonable to consider this second term as a perturbation. All quantities pertaining to the "unperturbed" $4/r^{12}$ problem will be denoted by the superscript 0. Developing the exponential for the perturbation terms one easily obtains[11]

$$Q_N = Q_N^{(0)}\{1 - \beta\langle \mathcal{U}\rangle_0 + \tfrac{1}{2}\beta^2\langle \mathcal{U}^2\rangle_0 + \cdots\}, \tag{3}$$

where the brackets denote canonical average with respect to the unperturbed system, $\mathcal{U}$ stands for

$$\mathcal{U} = -\sum_{i<j} \frac{4}{r_{ij}^6}, \tag{4}$$

and $Q_N^{(0)}$, the unperturbed partition function, is given by

$$Q_N^{(0)} = \frac{1}{N!}\int_V \exp\left(-\beta \sum_{i<j} \frac{4}{r_{ij}^{12}}\right) d^3r_1 \cdots d^3r_N . \tag{5}$$

Taking the logarithm of Eq. (3), the free energy up to second order in the perturbation $\mathcal{U}$ reads

$$F = -\frac{1}{\beta}\log Q_N = F^{(0)} + \langle \mathcal{U}\rangle_0 - \tfrac{1}{2}\beta[\langle \mathcal{U}^2\rangle_0 - \langle \mathcal{U}\rangle_0^2] . \tag{6}$$

Differentiation of the free energy with respect to total volume and temperature yields the following expressions for the equation of state and the internal energy, up to first order in the perturbation:

$$\frac{\beta p}{\rho} = \frac{\beta p^{(0)}}{\rho} + \frac{2\beta}{N}\langle \mathcal{U}\rangle_0 - \frac{4\beta^2}{N} \times (\langle \mathcal{W}\cdot\mathcal{U}\rangle_0 - \langle \mathcal{W}\rangle_0\langle \mathcal{U}\rangle_0), \tag{7}$$

$$\mathfrak{u} = \mathfrak{u}^{(0)} = \langle \mathcal{U}\rangle_0 + \beta(\langle \mathcal{U}\cdot\mathcal{W}\rangle_0 - \langle \mathcal{U}\rangle_0\langle \mathcal{W}\rangle_0). \tag{8}$$

Here $\mathcal{U}$ is given by (4) and $\mathcal{W}$ is

$$\mathcal{W} = \sum_{i<j} \frac{4}{r_{ij}^{12}} . \tag{9}$$

The second-order terms for $\beta p/\rho$ and $\mathfrak{u}$, obtained by differentiation of the corresponding term of the free energy [i.e., the last term of the right-hand side of Eq. (6)], have a much more complicated structure (with fluctuation terms of third order), and their calculation by computer-"experimental" methods is hopeless. We shall not consider them here.

Consider now the unperturbed configurational partition function $Q_N^{(0)}$; changing to reduced distances

$$\vec{q}_i = \rho^{1/3}\,\vec{r}_i ,$$

we have

$$Q_N^{(0)} = \frac{V^N}{N!}\int_{\text{unit volume}} \exp\left(-4\,\beta\rho^4 \sum_{i<j} 1/q_{ij}^{12}\right) \times d^3q_1 \cdots d^3q_N . \tag{10}$$

The factor $V^N/N!$ is simply the ideal-gas contribution. Thus the excess free energy is simply a function of the variable $\beta\rho^4$, or its inverse TV^4, i.e.,

$$\beta F^{(0)}(\beta,\rho) = \log\rho - 1 + \chi^{(0)}(\beta\rho^4). \tag{11}$$

The first two terms of the right-hand side of Eq. (10) are the ideal-gas contribution to the configurational free energy.

Similarly the equation of state reads

$$\frac{\beta p^{(0)}}{\rho} = \rho \frac{\partial(\beta F^{(0)})}{\partial \rho} = 1 + 4\beta\rho^4 \chi^{(0)\prime}(\beta\rho^4)$$
$$= 1 + \pi^{(0)}(\beta\rho^4) . \quad (12)$$

Also, the internal energy is

$$\beta u^{(0)} = -T \frac{\partial}{\partial T}(\beta F^{(0)}) = \beta\rho^4 \chi^{(0)\prime}(\beta\rho^4)$$
$$= \frac{1}{4}\left(\frac{\beta p^{(0)}}{\rho} - 1\right) . \quad (13)$$

The primes denote first-order derivatives of the functions with respect to their argument.

If the perturbation term (4) is added, it can be easily seen that the first- and second-order corrections to the free energy [Eq. (6)] are likewise functions of $\beta\rho^4$:

$$\beta F^{(1)}(\beta,\rho) = \beta \langle v \rangle_0 = \beta^{1/2} \chi^{(1)}(\beta\rho^4) , \quad (14)$$

$$\beta F^{(2)}(\beta,\rho) = -\tfrac{1}{2}\beta^2[\langle v^2\rangle_0 - \langle v\rangle_0^2] = \beta \chi^{(2)}(\beta\rho^4) , \quad (14')$$

and similar relations for the corrections to the equation of state and the internal energy. (See note added in proof.)

Thus it clearly appears that calculating the thermodynamic properties for an inverse-12 potential system as well as the inverse-6 corrections along one isotherm is sufficient to determine these same properties for any temperature and density.

In order to have an idea of the convergence of the perturbation series for the free energy, we first made some cell-model calculations in the Lennard-Jones-Devonshire (LJD) approximation,[12] both for the inverse-12 and the complete LJ 12-6 potentials. The LJD cell-model approximation is known to yield reasonable results for the solid-state thermodynamic properties of systems with hard-core potentials[13] and moreover allows one to calculate very easily the free energy and equation of state as well as the first- and second-order corrections to the free energy. Some numerical results are gathered in Table I. They show that down to reduced temperatures of the order of 2.5, inclusion of the first two corrections gives good results for the free energy. These results can only be considered as a hint for a good convergence of the perturbation series in the high-density (solid-state) region. The convergence of the series in the fluid region can only be checked by direct numerical calculations based on computer experiments. This will be considered in Sec. III.

TABLE I. Convergence of the perturbation series in the LJD cell model $\beta F^{(0)}$, $\beta F^{(1)}$, and $\beta F^{(2)}$ are, respectively, the zero-, first-, and second- order contributions to the free energy divided by the temperature. The sum of these three terms is to be compared to βF, the free energy for the LJ potential, divided by the temperature.

T	ρ	$\beta F^{(0)}$	$\beta F^{(1)}$	$\beta F^{(2)}$	$\beta(F^{(0)}+F^{(1)}+F^{(2)})$	βF
100	2.6	8.131	− 1.061	−0.002	7.067	7.067
100	3.	11.043	− 1.370	−0.001	9.672	9.672
50	2.4	9.882	− 1.770	−0.003	8.109	8.108
50	2.8	14.169	− 2.349	−0.002	11.818	11.817
20	2	10.965	− 3.046	−0.007	7.912	7.911
20	2.4	17.201	− 4.278	−0.004	12.919	12.918
5	1.4	10.717	− 5.981	−0.030	4.706	4.702
5	1.8	20.212	− 9.575	−0.013	10.624	10.622
2.5	1.2	11.192	− 8.759	−0.057	2.376	2.366
2.5	1.4	16.350	−11.670	−0.036	4.644	4.638

III. NUMERICAL RESULTS

In order to investigate the high-temperature liquid-solid coexistence curve and transition data along the lines developed in Secs. I and II, we made extensive Monte Carlo calculations for the inverse-12 potential system along the isotherm $T = 100$. As already mentioned, similar computations have been carried through independently by Hoover and collaborators[5] and their results provide a direct check of our "unperturbed" transition data.

A. Fluid Phase Results

The low-density fluid thermodynamic properties were calculated using the familiar Percus-Yevick (PY)[14] integral equation for the radial distribution function; the PY results proved accurate up to densities of the order of 0.7. At higher densities the equation of state and other thermodynamic properties were computed by the Metropolis Monte Carlo method[6] applied to a system of 864 atoms enclosed in a cubic box with periodic boundary conditions. For intermediate densities, about 6×10^5 configurations were generated during each run, and about 10^6 for the highest densities. The successive runs were carried through for states whose densities differed generally by 0.1 or 0.2. Thus, the fluid was gradually compressed and the initial configuration for a given density was obtained by scaling the interparticle distances from the final configuration of the preceding run. In each run, the first $1-2\times10^5$ configurations generated were not included in the calculation of the thermodynamic averages in order to obtain a faster convergence towards "equilibrium". The following properties were computed by averaging over the remaining configurations: the equation of state $\beta p^{(0)}/\rho$, the internal energy

$$u^{(0)} = \langle \sum_{i<j} 4/r_{ij}^{12} \rangle ,$$

the first-order correction to the free energy [Eq. (14)], the second-order correction to the free energy [Eq. 14′)], and the first-order correction to the equation of state [Eq. (7)]. The first three properties, which can be simply evaluated with

the help of the radial distribution function, are obtained with an accuracy of the order of 1% or better by the Monte Carlo procedure; the last two quantities which are related to fluctuations of $\mathcal{U}$ [Eq. (4)] and $\mathcal{W}$[Eq. (9)] are only obtained with an accuracy of the order of 30%, but this is not an important drawback as we shall see. The essential numerical results of our computations for the fluid isotherm are gathered in Table II. The equation of state for the "unperturbed" system (i.e., the $4/r^{12}$ potential) can be written as a simple polynomial in $\beta^{1/4}\rho$ [remember Eq. (12)] which fits the Monte Carlo data very well. The best fit is obtained for the following polynomial:

$$\beta p^{(0)}/\rho - 1 = B_1\beta^{1/4}\rho + B_2\beta^{1/2}\rho^2 + B_3\beta^{3/4}\rho^3 + B_4\beta\rho^4 + B_{10}\beta^{10/4}\rho^{10}, \quad (15)$$

with $B_1 = 3.629$, $B_2 = 7.2641$, $B_3 = 10.4924$, $B_4 = 11.459$, $B_{10} = 2.176\,19$.

While fitting the equation of state, the coefficient of ρ was kept fixed and equal to the second virial coefficient:

$$B_1\beta^{1/4} = \tfrac{1}{3}(2^{3/2}\pi)\,\Gamma(\tfrac{3}{4})\beta^{1/4}. \quad (16)$$

Equation of state (15) allows a direct comparison of our data with the results of Hoover *et al.*[5] obtained for $T = 1$. Table III summarizes the comparison. The difference between both sets of values never exceeds 1% which represents roughly the combined errors; as both sets of values are actually smoothed results, the agreement can be considered as excellent.

TABLE II. Fluid phase thermodynamic results along the isotherm $T = 100$ for the inverse-12 potential. $\beta\mathcal{U}$ is the internal energy divided by the temperature $\beta p/\rho$ the equation of state; $\beta F^{(0)}$, the configurational part of the free energy divided by the temperature [Eq. (17)]; $\beta F^{(1)}$, the first-order correction to the free energy due to the inverse-6 part of the LJ potential divided by the temperature [Eq. (14)]. The data at the lower densities (up to $\rho = 0.6$) were calculated with the help of the PY equation. All other data are Monte Carlo results.

ρ	$v = 1/\rho$	$\beta\mathcal{U}$	$\beta p/\rho$	$\beta F^{(0)}$	$-\beta F^{(1)}$
0.1	10	0.0306	1.122	−3.18	0.0176
0.2	5	0.0654	1.261	−2.36	0.0368
0.3	3.333	0.105	1.419	−1.82	0.0574
0.4	2.5	0.149	1.597	−1.39	0.0795
0.5	2	0.199	1.797	−1.01	0.103
0.6	1.666	0.255	2.021	−0.66	0.128
0.7	1.429	0.327	2.307	−0.33	0.157
0.8	1.25	0.403	2.612	0	0.187
0.9	1.111	0.485	2.94	0.32	0.218
1	1	0.577	3.31	0.65	0.251
1.2	0.833	0.807	4.23	1.33	0.324
1.4	0.714	1.100	5.40	2.06	0.407
1.6	0.625	1.457	6.83	2.87	0.498
1.8	0.555	1.880	8.52	3.77	0.597
2	0.5	2.424	10.70	4.78	0.707
2.3256	0.43	3.57	15.28	6.71	0.908
2.5	0.4	4.31	18.23	7.92	1.025
2.7	0.37	5.36	22.45	9.48	1.171

TABLE III. Comparison between the equation-of-state data (inverse-12 potential) calculated from Eq. (15) for $T = 1$ and the results of Hoover *et al.* (Ref. 5).

ρ	$\beta p/\rho$ from (15)	$\beta p/\rho$ from Ref. 5
0.1	1.447	1.448
0.2	2.118	2.121
0.4	4.578	4.557
0.6	9.556	9.460
0.7	13.511	13.469
0.8	18.851	18.762

The "unperturbed" configurational free energy per atom is obtained by simply integrating (15):

$$\beta F^{(0)}/N = \int_0^\rho (\beta p^{(0)}/\rho' - 1)\,d\rho'/\rho' + \log\rho - 1. \quad (17)$$

The first-order correction to the free energy [Eq. (14)] can also be easily fitted by a polynomial in $\beta^{1/4}\rho$:

$$\beta F^{(1)}/N = -\beta^{1/2}[C_1\beta^{1/4}\rho + C_2\beta^{1/2}\rho^2 + C_3\beta^{3/4}\rho^3 + C_4\beta\rho^4 + C_5\beta^{5/4}\rho^5], \quad (18)$$

with $C_1 = 5.3692$, $C_2 = 6.5797$, $C_3 = 6.1745$, $C_4 = -4.2685$, $C_5 = 1.6841$.

The corresponding first-order corrections to the equation of state and the internal energy are then obtained by simple differentiation of (18) with respect to the density or the temperature. In fact the calculation of the correction terms by this procedure is much more precise than the direct evaluation of the fluctuation terms present in Eqs. (7) and (8) and which are obtained by the Monte Carlo method with a precision of only about 30%.

Lastly, we must consider the second-order correction to the free energy, as given by Eq. (14′). Again, because it is a fluctuation term it cannot be calculated with a high precision within reasonable computer times. But our Monte Carlo computations yield rough values of this term which show that it is small compared to the first-order perturbation term and also slowly varying with the density. More precisely, for $T = 100$, $\rho = 2$, we find $\beta F^{(0)} = 4.78$; $\beta F^{(1)} = -0.71$; $\beta F^{(2)} \simeq -0.003$ (see Table III). At that temperature $\beta F^{(2)}$ varies between the extreme (approximate values) −0.002 and −0.004 over the whole density range. The value $\simeq -0.004$ is reached in the vicinity of $\rho = 1.6$ and the correction (which is of course always negative) increases below and above that density.

For $T = 5$, $\rho = 1$, the corresponding values are easily calculated by the above-mentioned scaling

procedure [Eqs. (11), (14), and (14′)]; we find

$$\beta F^{(0)} = 4.67, \quad \beta F^{(1)} = -3.46, \quad \beta F^{(2)} \simeq -0.05.$$

The two results given for $T = 100$ and $T = 5$ seem to indicate a strong convergence of the perturbation series over the whole high-temperature range. This view is supported by close inspection of the results at all densities. It should be stressed however that the second-order corrections to the equation of state and internal energy cannot be obtained by numerical differentiation of the free-energy second-order correction as the precision of its computed values is very poor as already mentioned. Nevertheless, the slow variation of $\beta F^{(2)}$ with density at fixed temperature ensures that its derivative and hence the second-order correction to the equation of state must also remain small as compared to the first-order correction.

Another and more conclusive method to check the convergence of the perturbation series is a direct comparison of its predictions with an exact Monte Carlo calculation of the thermodynamic properties for a system of atoms interacting through the complete LJ potential. At low densities the PY results are also helpful. A certain number of high-temperature Monte Carlo results for LJ systems of 32 or 108 atoms have been published by Wood[15] for the three temperatures $T = 5$, 20, and 100. We have complemented those data by some PY calculations and by Monte Carlo calculations. We have also compared the perturbation results with the LJ Monte Carlo results along the isotherm $T = 2.74$, which were published in I. This temperature cannot be considered as "high" (for comparison we recall that the critical temperature for LJ systems is approximately 1.35) and we do not expect *a priori* the perturbation series to yield very good results at that tempera-

TABLE IV. Comparison of LJ thermodynamic properties from exact calculations (superscript ex) and from first-order perturbation theory (superscript per). $\beta p/\rho$ is the equation of state, $\beta \mathfrak{U}$ the internal energy divided by the temperature, βF the configurational free energy divided by the temperature. In the last column the labels indicate the source of the exact LJ calculations: PY are Percus-Yevick equation results, MC are our own Monte Carlo computations, and *W* are the Monte Carlo computations of Wood (Ref. 15).

T	ρ	$(\beta p/\rho)^{ex}$	$(\beta p/\rho)^{per}$	$(\beta \mathfrak{U})^{ex}$	$(\beta \mathfrak{U})^{per}$	$(\beta F)^{ex}$	$(\beta F)^{per}$	Label
100	0.2	1.221	1.221	0.036	0.037	−2.40	−2.40	PY
	0.4	1.505	1.506	0.085	0.087	−1.47	−1.47	PY
	0.5	1.675	1.679	0.115	0.118	−1.11	−1.11	PY
		(1.671)		(0.114)				(W)
	0.666	2.007	2.022	0.175	0.181	−0.59	−0.58	PY
		(2.002)		(0.175)				(W)
	1	2.95	2.97	0.361	0.367	0.39	0.39	W
	1.333	4.36	4.41	0.648	0.664	1.42	1.43	W
	1.4	4.76	4.77	0.734	0.740	1.65	1.66	MC
	2	9.50	9.56	1.767	1.786	4.05	4.07	W
	2.222	12.10	12.23	2.346	2.388	5.18	5.21	W
	2.38	14.46	14.54	2.887	2.913	6.09	6.13	W
	2.5	16.29	16.52	3.304	3.367	6.84	6.89	W
20	0.2	1.270	1.274	−0.005	0.004		−2.35	PY
	0.4	1.667	1.675	0.009	0.025		−1.36	PY
	0.5	1.930	1.945	0.026	0.045		−0.96	PY
		(1.888)		(0.021)				(W)
	0.666	2.508	2.538	0.083	0.104		−0.32	W
	1	4.458	4.50	0.348	0.374		1.03	W
	1.333	7.999	8.08	0.942	0.984		2.77	W
	1.765	16.68	16.73	2.65	2.67		6.06	MC
5	0.2	1.169	1.199	−0.202	−0.139		−2.43	PY
	0.5	1.867	1.869	−0.474	−0.389		−1.12	PY
		(1.865)		(−0.468)				(W)
	0.666	2.628	2.70	−0.584	−0.492		−0.48	W
	1	6.336	6.45	−0.456	−0.370		1.20	W
	1.279	13.44	13.40	0.435	0.468		3.51	MC
2.74	0.2	0.992	1.052	−0.440	−0.293	−2.65	−2.55	PY
	0.4	1.20	1.22	−0.865	−0.686	−1.93	−1.78	MC
	0.7	2.59	2.56	−1.424	−1.291	−0.98	−0.85	MC
	0.8	3.61	3.60	−1.562	−1.428	−0.57	−0.45	MC
	0.9	5.14	5.11	−1.609	−1.492	−0.06	0.05	MC
	1	7.37	7.23	−1.525	−1.452	0.58	0.69	MC
	1.1	10.17	10.15	−1.351	−1.259	1.41	1.51	MC

ture. We have nevertheless made the comparison because the LJ data along the 2.74 isotherm are rather complete, which is not true of the higher isotherms. The data along the isotherms $T=5$ and $T=20$ taken from Wood and our own PY and Monte Carlo computations are insufficient to allow for a calculation of the free energy through Eq. (17). For $T=100$, results are also somewhat scarce but sufficient for a rather unprecise evaluation of the free energy (the error should however not exceed 1%). In Table IV the thermodynamic data from first-order perturbation theory and from the exact LJ computations are compared for the above-mentioned temperatures. At $T=100$ there seems to be no significant difference between the exact and the perturbation results, except at the highest densities. But we believe the slight discrepancies at those densities to be due to the inaccuracy of the equation-of-state results from Wood's work which appear to be systematically too low especially at high density, for each of the three isotherms. This view is supported by a close investigation of Wood's data in the vicinity of our own results, e.g., the points ($T=100$, $\rho=1.4$), ($T=20$, $\rho=1.765$), ($T=5$, $\rho=1.279$) and also the PY point ($T=20$, $\rho=0.5$). At $T=20$ the PY result is certainly very precise at the relatively low density 0.5; as a matter of fact the PY result for the equation of state can only be lower than the exact result, but here the converse is true which indicates that Wood's value is certainly too low at that particular density. The reason for the apparently systematic error in Wood's equation-of-state data can be due either to the relatively small size of his systems (32 or 108 atoms as compared to our 864), or to an inadequate choice of the initial configuration (which is generally an fcc lattice according to Ref. 15).

Bearing this restriction in mind, we see in Table IV that the perturbation results are in very good agreement with the exact LJ results for $T=100$ and $T=20$; the agreement is still reasonable at $T=5$ and even, rather unexpectedly, at $T=2.74$, except for the internal energy values. At $T=2.74$ the difference between the free energies obtained by the perturbation method and the LJ calculations is roughly equal to the second-order perturbation correction which was not included in the perturbation results (limited to first order as already mentioned). At that temperature the equation-of-state results are worst at low density, which is not a major drawback as we are essentially interested in high-density results.

Thus, it is clear that combining Eqs. (15) and (18) we obtain an equation of state for the LJ fluid which is very accurate in the high-temperature limit and provides an excellent extension of the equation of state proposed by Levesque and Verlet,[16] based on the Barker-Henderson[17] perturbation theory, which holds for low and intermediate temperatures (up to two or three times the critical temperature). The high-temperature equation of state, which yields already reasonable results at roughly twice the critical temperature is rather simple and finally reads

$$\begin{aligned}\beta p/\rho &= \beta p^{(0)}/\rho + \beta p^{(1)}/\rho = 1 + B_1\beta^{1/4}\rho \\ &+ B_2\beta^{1/2}\rho^2 + B_3\beta^{3/4}\rho^3 + B_4\beta\rho^4 + B_{10}\beta^{5/2}\rho^{10} \\ &- \beta^{1/2}[C_1\beta^{1/4}\rho + 2\times C_2\beta^{1/2}\rho^2 + 3\times C_3\beta^{3/4}\rho^3 \\ &+ 4\times C_4\beta\rho^4 + 5\times C_5\beta^{5/4}\rho^5], \end{aligned} \tag{19}$$

where the B's and C's are given below Eqs. (15) and (18).

B. Solid-Phase Results

As pointed out in the Introduction, the free energy of the solid phase (which we shall need in order to determine the coexistence curve) can be calculated by integrating the "single-occupancy" (or exact cell-model) equation of state for all densities. Just as for the fluid, we computed the single-occupancy thermodynamic properties for the inverse-12 (unperturbed) potential system along the isotherm $T=100$. The results in the "unphysical" region (i.e., below the melting density) are not given here. In Table V, the results in the solid phase (i.e., for those densities where the single-occupancy restriction is not operating any more because the atoms remain localized all by themselves) are presented. In addition to the equation of state, the internal energy, the free energy, and the perturbation terms, the mean square deviation of an atom from its lattice site has been computed:

$$S^2 = \frac{1}{N}\Big\langle \sum_i (\vec{r}_i - \vec{R}_i)^2 \Big\rangle_0. \tag{20}$$

Just as in the case of the fluid, the convergence of the perturbation series is strong at high temperatures. The second-order correction to the free energy is of the same order of magnitude as in the high-density fluid. The comparison with the LJ data at $T=2.74$ again shows reasonable agreement between these data and the perturbation results,

TABLE V. Solid-phase results for the inverse-12-potential ($T=100$). The meaning of the symbols is the same as in Table II. S^2 is the mean-square deviation of an atom from its lattice site [Eq. (20)].

ρ	$v=1/\rho$	$\beta\mathfrak{U}$	$\beta p/\rho$	$\beta F^{(0)}$	$-\beta F^{(1)}$	S^2
2.6	0.385	4.19	17.78	8.69	1.064	0.185×10^{-1}
2.8	0.357	5.15	21.61	10.14	1.210	0.113×10^{-1}
3	0.333	6.36	26.45	11.79	1.371	0.78×10^{-2}

except at very high density where the discrepancies between the equation-of-state and free-energy values become more important. This is not troublesome however as we are primarily interested in the melting properties, and consequently the lowest solid densities.

C. Phase Transition

Having calculated the free energies of the fluid and the solid, we are now in a position to determine the transition densities and pressure by the Maxwell double-tangent construction in exactly the same way as was done in I. This was first done for the inverse-12 potential problem; because of the scaling properties [Eq. (11)], the densities of the coexisting phases and the transition pressure are simple functions of the temperature:

$$\rho_S = 0.844\ (\pm 0.002) \times \beta^{-1/4}\ ,$$
$$\rho_L = 0.814\ (\pm 0.002) \times \beta^{-1/4}\ , \qquad (21)$$
$$P_m = 16.0\ \ (\pm 0.1) \times \beta^{-5/4}\ ,$$

where ρ_S is the density of the solid at melting, ρ_L the volume of the coexisting liquid phase, and P_m the melting pressure. These numerical values are in remarkable agreement with those given by Hoover *et al.*[5] which are, respectively, 0.844, 0.813, and 15.95.

If now the first-order correction is added to the free energy, the double-tangent construction can be repeated for the LJ system at various temperatures. The results are summarized in Table VI which gives the transition densities and pressures for $T = 100$, 50, 20, 10, 5, and 2.74 both for the unperturbed inverse-12 system [formulas (21)] and for the LJ system in the first-order approximation. Because of the strong convergence of the free-energy perturbation series, the first-order results are expected to be very close to the exact LJ results. This is confirmed at the lowest (least favorable) temperature considered ($T = 2.74$), by a direct comparison with the exact LJ result from I, i.e., $\rho_L = 1.113$ (against 1.117), $\rho_S = 1.179$ (against 1.191), and $P_m = 32$ (against 33). Consequently, one can be very confident about the perturbation results at higher temperatures. The LJ coexistence curve is shown in Fig. 1 (with a logarithmic scale for the temperatures) compared to the inverse-12 coexistence curve. The transition data from I were used for the low-temperature region.

TABLE VI. Liquid-solid transition densities and pressures for the inverse-12 potential and the LJ potential (from first-order perturbation theory). ρ_L and ρ_S are the liquid and solid densities along the coexistence curve and P the transition pressure.

		Inverse-12 potential			LJ potential		
T	$\beta = 1/T$	ρ_L	ρ_S	P	ρ_L	ρ_S	P
100	0.01	2.570	2.670	5050	2.601	2.706	4800
50	0.02	2.162	1.246	2170	2.200	2.291	1970
20	0.05	1.720	1.785	675	1.765	1.843	590
10	0.1	1.447	1.501	282	1.500	1.572	231
5	0.2	1.216	1.262	120	1.279	1.349	86
2.74	0.365	1.047	1.086	56	1.117	1.191	33

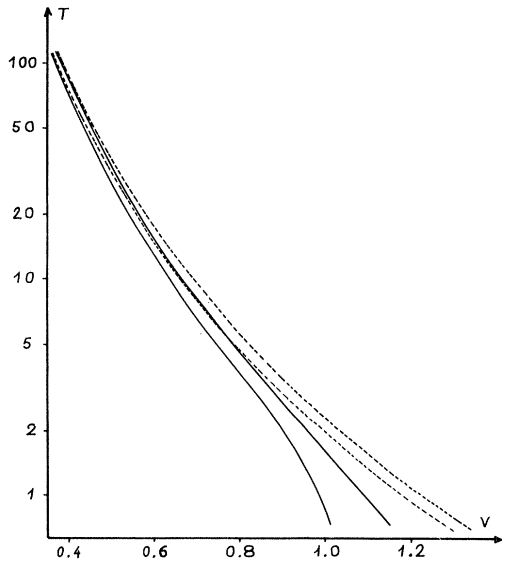

FIG. 1 Coexistence curve for the inverse-12 potential system (broken curve) and the LJ system (full curve). V is the reduced volume per atom, T the temperature (on a logarithmic scale).

IV. MELTING AND CRYSTALLIZATION CRITERIA

In this section, we shall investigate a well-known melting criterion, i.e., the familiar Lindemann melting law, and the crystallization criterion based on the magnitude of the structure-factor maximum, which was introduced in I.

It is first of all clear that the Lindemann law is actually exact for systems of atoms interacting through a repulsive potential which is homogeneous in the coordinates of all the atoms and in particular for the inverse-12 potential; this is again a consequence of the scaling properties valid for homogeneous potentials, which ensure that the product $S^2 \times \rho^{2/3}$ is a constant along the melting curve; this is the most direct formulation of Lindemann's law (for a detailed discussion of this law see Ref. 18). S^2 was computed along the solid-phase isotherm of the inverse-12 problem, as mentioned earlier. If ρ_m and T_m denote the melting density and temperature and a_m is the nearest-neighbor distance at melting ($a_m = 2^{1/6}/\rho_m^{1/3}$), the Lindemann constant according to our Monte Carlo computations is

$$S^2(T_m, \rho_m)/a_m^2 = 0.023 \pm 0.001. \quad (22)$$

The square root of the corresponding inverse ratio $\eta_m = a_m/S_m$ equals 6.6.

As the inverse-12 problem represents a good zero-order approximation to the complete LJ problem at high temperature, we expect the Lindemann law to be approximately valid for LJ systems, with possibly a different value of the Lindemann constant. We checked this for the lower temperature range considered in I. The situation is pictured in Fig. 2 where the solid curves represent S^2 as a function of $a^2 = 2^{1/3}/\rho^{2/3}$ along four isotherms ($T = 0.75$, 1.15, 1.35, and 2.74). The vertical broken lines correspond to the values of a^2 at melting (i.e., a_m^2) for these four temperatures. The intersections of these vertical lines with the S^2 curves determine the values of the ratios $\eta_m = a_m/S_m$ at melting. These values are

$$T = 0.75, \quad \eta_m = 6.87; \quad T = 1.15, \quad \eta_m = 7.18;$$
$$T = 1.35, \quad \eta_m = 7.28; \quad T = 2.74, \quad \eta_m = 6.72.$$

Thus, the fraction η_m turns out to be remarkably constant within the statistical errors (about 5% on the S^2 values). The broken curve in Fig. 2 corresponds to the situation where Lindemann's law would be verified exactly for the constant value $\eta_m = 7$. The deviation of this "ideal" case from our results is hardly significant due to the rather large error bars. Thus it can be safely concluded that Lindemann's melting law holds for the classical LJ solid over a wide temperature range.

The crystallization criterion, based on the analogy with the hard-sphere system, states that the fluid crystallizes whenever the maximum value of the structure factor $S(k_0)$ reaches a certain constant value. We recall that the structure factor is defined by

$$S(k) = \sum_{i,j} \frac{\langle e^{i\vec{k}(\vec{r}_i - \vec{r}_j)} \rangle}{N} \quad (23)$$

and is simply related to the Fourier transform of the radial distribution function. In I, this law was discussed in more detail and shown to hold for the LJ system in the temperature range considered there with a constant maximum value $S(k_0)$ equal to 2.85. Here we are interested in the extension of the law to the high-temperature limit.

Just as in the case of the Lindemann law, it is a straightforward matter to show that the structure factor "law" is exact in the case of a homogeneous potential. Indeed, applying the scaling property for such a potential to the definition of the radial distribution function, one obtains the relation

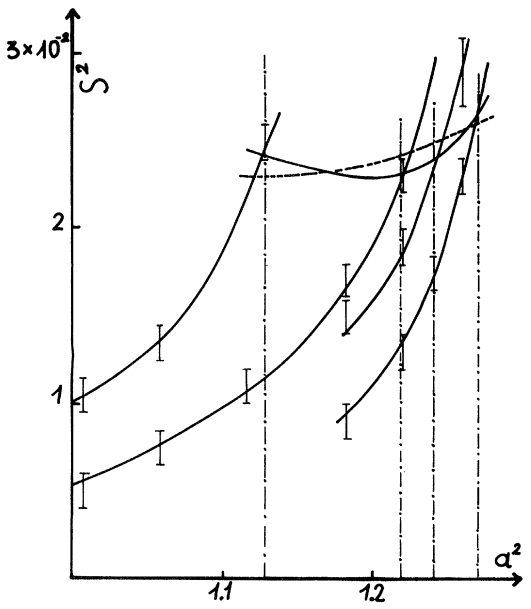

FIG. 2. Mean-square deviation S^2 of an atom from its lattice site as a function of the square of the nearest-neighbor distance a^2 along the isotherms $T = 0.75$, 1.15, 1.35, and 2.74 (upper left curve). The broken vertical lines correspond to the four melting densities. The S^2 data are taken from Refs. 4 and 13.

$$g_{\lambda^n T, \lambda^3 V}(\lambda r) = g_{T,V}(r). \quad (24)$$

Here λ is the scaling coefficient and n is the exponent of the potential $v(r) = r^n$ ($n = -12$ in our case).

Hence, the structure factor, obtained by Fourier-transforming $g - 1$, verifies

$$S_{\lambda^n T, \lambda^3 V}(k/\lambda) = S_{T,V}(k). \quad (25)$$

Now, if the state (T, V) lies on the fluid branch of the coexistence curve, then the same is true of all the states $(\lambda^n T, \lambda^3 V)$ $(0 < \lambda < \infty)$ according to the relations (21) (where $n = -12$). This completes the proof of the statement that at crystallization $S(k)$ is always the same except for the scaling of the wave vector. In fact this property of homogeneous potential systems is not surprising because there is no temperature-independent characteristic length in such systems. This is not true of more general potentials and in particular of the LJ potential. But again a similar law can be expected to hold approximately for LJ systems because of the essentially geometric properties underlying the structure-factor law. (cf. the discussion in I.) For the inverse-12 problem the maximum of the structure factor at crystallization turns out to be $S(k_0) = 2.95 \pm 0.05$ from the Monte Carlo computations. Taking for the crystallization densities of the LJ fluid the values obtained by our perturbation calculation (Table VI), we calculated the

structure factor at $T=5$, $\rho_L=1.279$ and $T=20$, $\rho_L=1.765$. The corresponding maxima are 2.9 ± 0.05 and 2.95 ± 0.05.

Taking into account both the statistical errors and the small uncertainties on the transition densities due to their determination by perturbation theory, these results show that the law $S(k_0) \simeq 2.85$ at crystallization can be extended to the high-temperature region for LJ systems, with perhaps a very weak temperature dependence of the maximum.

The small temperature dependence of the structure factor maximum at crystallization seems to indicate that at high temperature the analogy of the LJ fluid with an "equivalent" hard-sphere fluid is not as close as for lower temperatures. We recall that at crystallization $S(k_0)=2.85$ for the hard-sphere fluid. Our results seem to indicate a tendency towards a higher maximum as the temperature increases. Actually the complete structure factor for the inverse-12 system does not fit the equivalent hard-sphere structure factor as well as the low-temperature LJ structure factor does. For example, for $T=100$ and $\rho=2.5$ the height of the second peak is 0.38 as compared to 0.26 for the equivalent hard-sphere system. The discrepancies are possibly due to the fact that at high temperatures, it is difficult to define a well-determined equivalent hard-sphere diameter. This is probably related to the difficulties of the Barker-Henderson perturbation theory at high temperatures which will be briefly discussed in Sec. V.

V. DISCUSSION

The high-temperature perturbation method based on the separation of the LJ potential into its two homogeneous parts, and which was initially devised for rather practical reasons, turns out to be a good approach to the LJ problem even at intermediate temperatures. Our perturbation approach avoids the difficulties encountered by the Barker-Henderson perturbation theory at high temperatures as shown by the work of Levesque and Verlet.[16] The starting point of the Barker-Henderson theory is the hard-sphere system and the difficulty at high temperatures lies essentially in the definition of the equivalent hard-sphere diameter. Recently these authors have suggested a variational method to determine the "best" hard-sphere diameter for a given density and temperature of the LJ system.[19] Taking the inverse-12 potential as a starting point avoids this difficulty from the beginning and represents an alternative zero-order approximation to the LJ problem.

Terminating the perturbation series after first order yields good results down to a reduced temperature of about 5. The next term of the series has been shown to be small and of the same order as the difference between the exact LJ data and the perturbation results. Important progress would thus be achieved if the second-order fluctuation term could be calculated with a good precision. This is in principle possible by the Monte Carlo method, but much faster computers would be necessary for actual computations. Approximate expressions for the fluctuation terms, of the type proposed by Barker and Henderson, unfortunately yield very inaccurate results.[16]

Finally, both the Lindemann and the structure-factor laws turn out to give reasonable estimates of the fluid-solid transition densities. Close inspection of the structure factor in the high-temperature limit indicates that the high-temperature LJ fluid is less well approximated by an equivalent hard-sphere fluid than in the low-temperature region. This is a consequence of the fact that at high temperature the distance of closest approach between two atoms is smaller and the potential felt in a collision varies more widely as the temperature increases, which renders a clear definition of the equivalent hard-sphere diameter more difficult.

Note added in proof. Thus βF for the LJ potential appears as a function of the variables $\beta^{1/2}$ and $\beta^{1/4}\rho$. In fact, J. L. Lebowitz [Phys. Letters 28A, 596 (1969)] has shown that in a properly defined domain the thermodynamic properties for the LJ potential are analytic in these two variables.

ACKNOWLEDGMENTS

The author is deeply indebted to D. Levesque for his constant help and advice in large parts of the numerical work. The author also acknowledges clarifying discussions with L. Verlet. Professor W. Hoover kindly provided a copy of the manuscript of his forthcoming paper on the soft-sphere equation of state (see Ref. 5).

*Laboratoire associé au Centre National de la Recherche Scientifique. Present address: Laboratoire de Physique Théorique et Hautes Energies, Bâtiment 211, Faculté des Sciences, 91-Orsay, France.

[1]B. J. Alder and T. E. Wainwright, Phys. Rev. 127, 359 (1962).

[2]W. G. Hoover and F. H. Ree, J. Chem. Phys. 47, 4873 (1967).

[3]W. G. Hoover and F. H. Ree, J. Chem. Phys. 49, 3609 (1968).

[4]J.-P. Hansen and L. Verlet, Phys. Rev. 184, 151 (1969).

[5]W. G. Hoover, M. Ross, K. W. Johnson, D. Henderson, J. A. Barker, and B. C. Brown, J. Chem. Phys. (to be published).

[6]N. A. Metropolis, A. W. Rosenbluth, M. N. Rosenbluth, A. H. Teller, and E. Teller, J. Chem. Phys. 21, 1087 (1953); W. W. Wood and F. R. Parker, J. Chem. Phys. 27, 720 (1957).

[7]A. Rahman, Phys. Rev. 136, A405 (1964); L. Verlet, Phys. Rev. 159, 98 (1967).

[8]A. Michels, H. Wijker, and H. K. Wijker, Physica 15, 627 (1949).

[9]J. S. Brown, Proc. Phys. Soc. (London) 89, (1966).

[10]J.-P. Hansen and J. J. Weis, Phys. Rev. 188, 314 (1969).

[11]L. D. Landau and E. M. Lifshitz, *Statistical Physics* (Pergamon, New York, 1959), p. 93; R. W. Zwanzig, J. Chem. Phys. 22, 1420 (1954).

[12]T. L. Hill, *Statistical Mechanics* (McGraw-Hill, New York, 1956), p. 376.

[13]J.-P. Hansen, Orsay Report No. 69/46, 1969 (unpublished).

[14]J. K. Percus and G. J. Yevick, Phys. Rev. 110, 1 (1958).

[15]W. W. Wood, in *Physics of Simple Liquids*, edited by H. N. V. Temperley, J. S. Rowlinson, and G. S. Rushbrooke (North-Holland, Amsterdam, 1968), p. 116.

[16]D. Levesque and L. Verlet, Phys. Rev. 182, 307 (1969).

[17]J. S. Barker and D. Henderson, J. Chem. Phys. 47, 4714 (1967).

[18]M. Ross, Phys. Rev. 184, 233 (1969).

[19]D. Henderson and J. A. Barker, Phys. Rev. Letters (to be published).

PHYSICAL REVIEW A VOLUME 2, NUMBER 1 JULY 1970

Systematic Approach to the Bose Liquid

M. Schwartz

Soreq Nuclear Research Centre, Yavne, Israel

(Received 10 October 1969)

An approximation scheme for a Bose liquid is presented, based on small fluctuations in density and currents. The method of obtaining the elementary excitations and their interactions in any order of the approximation is outlined. Also it is shown that the first-order calculations are in agreement with the calculations of Feynman, Bogoliubov, and Pitayevski. Second-order calculations agree with the improved results of Feynman and Cohen.

I. INTRODUCTION

In this paper, a systematic approximation scheme for the interacting Bose liquid is derived. The method used is based on the assumption of small fluctuations of the density operator $\rho(r)$ and the current operator $J(r)$ from their averages. It differs, however, in several important aspects from Pitayevski's coarse-grained theory, which is based on a similar idea.[1] In Sec. II the Hamiltonian is expressed in terms of the current and density operators, and the commutation relations of the Fourier transforms of these operators are derived. Section III uses the assumption of small fluctuations of ρ and J from their average values in order to approximate the commutation relations, as well as the Hamiltonian. This first-order calculation yields the results of three apparently different theories: the Bogoliubov microscopic theory,[2] the Feynman variational theory,[3] and the Pitayevski theory. In Sec. IV the commutation relations and Hamiltonian are treated in a higher-order approximation. The procedure for obtaining the elementary excitations is discussed; it is easily shown that the wave functions obtained, in this order, are the Feynman-Cohen wave functions.[4,5] Higher-order expansions are discussed in Sec. V. The method for systematically deriving, the quasiparticle interactions without using phenomenological models is outlined, though actual calculations of this kind are postponed for later publication. Some general results holding for any order of the expansion are also explicitly derived in Sec. V.

II. HAMILTONIAN AND COMMUTATION RELATIONS

The Hamiltonian for a system of N identical bosons contained in a box of volume Ω and interacting via a two-body potential $v(r)$ is given by Eq. (1) ($\hbar = m = 1$):

$$H = \tfrac{1}{2}\int \nabla\psi^{\dagger}\cdot\nabla\psi d^3r + \tfrac{1}{2}\int \psi^{\dagger}(r)\psi^{\dagger}(r')\,v(r-r') \times\psi(r)\psi(r')\,d^3r d^3r' , \quad (1)$$

where $\psi^{\dagger}(r)$ and $\psi(r)$ are creation and destruction operators, respectively, of a particle at point r